

## Systematic studies of SiGe/Si islands nucleated via separate *in situ*, or *ex situ*, Ga<sup>+</sup> focused ion beam-guided growth techniques

T. E. Vandervelde<sup>1</sup>, S. Atha<sup>3</sup>, T. L. Pernelle<sup>2</sup>, R. Hull<sup>3</sup>, and J.C. Bean<sup>2\*</sup>

<sup>1</sup>Department of Physics, University of Virginia, 382 McCormick Road, Charlottesville, VA 22904, USA,

<sup>2</sup>Department of Electrical and Computer Engineering, University of Virginia, 351 McCormick Road, Charlottesville, VA 22904, USA

<sup>3</sup>Department of Materials Science, University of Virginia, 116 Engineers Way, Charlottesville, VA 22904, USA

\* Email: jcb6t@virginia.edu

### ABSTRACT

In this study we use 25keV *in situ* and 30keV *ex situ* Ga<sup>+</sup> focused ion beams (FIB) to locally modify the substrate before deposition to determine its affect on nucleation of MBE-grown Ge/Si islands. FIB processing may alter island formation in at least four ways: the surfactant effect of Ga<sup>+</sup>, doping effects of subsurface Ga<sup>+</sup>, crystalline damage, and surface roughening. To explore these possibilities, we milled square regions of increasing Ga<sup>+</sup> doses and used AFM to monitor islanding in and around these regions. For *in situ* experiments, doses ranged from  $\sim 10^{13}$  to  $5 \times 10^{17}$  ions/cm<sup>2</sup>. We began to observe changes in island topology at doses as low as  $\sim 10^{14}$  ions/cm<sup>2</sup>. For doses of  $\sim 10^{15}$  ions/cm<sup>2</sup> to  $\sim 8 \times 10^{16}$  ions/cm<sup>2</sup>, implanted areas were surrounded by denuded zones that grew from  $\sim 0.5$  to  $6 \mu\text{m}$ . Immediately inside the implanted area, island concentration (size and density) appeared to peak. At doses above  $\sim 6 \times 10^{16}$  ions/cm<sup>2</sup>, Ga<sup>+</sup> produced noticeable surface depressions, which were often surrounded by enhanced island densities, rather than a denuded zone. For *ex situ* FIB patterning, samples underwent both pre-growth cleaning and growth of a thin capping layer. Doses ranging from  $7.5 \times 10^{13}$  to  $\sim 10^{17}$  ions/cm<sup>2</sup> were used with varied capping layer thicknesses to study their combined affect on island nucleation. The results correspond well with *in situ* experiments for thin capping layers. Increased capping layer thickness show muted modifications for low Ga<sup>+</sup> doses, while for higher doses trends similar to the *in situ* results are seen.

### I: BACKGROUND:

Epitaxial growth of SiGe over Si (001) has been extensively studied.<sup>(1-14)</sup> This system is known to follow the Stranski-Krastanov mode of growth, with 60° misfit dislocations and 3-D islanding playing critical roles in relieving the strain energy that builds up due to the lattice mismatch between the substrate and the film. The different stages in islanding include the formation of pyramidal hut clusters with <501> facets, followed by formation of larger dome islands with primarily [201] and [311] facets, and finally enlargement of the domes through introduction of 60° misfit dislocation. Several groups have studied the transition between the different stages of island growth. Floro, *et al.* showed in their recent work<sup>(11)</sup> that strain-driven roughening behavior in low mismatch (low x for Si<sub>1-x</sub>Ge<sub>x</sub>) cases is qualitatively the same as that at much higher strains, including that for Ge on Si (001) with a mismatch of 4.2%. The transition of hut cluster to dome morphology has been explained by Ross, *et al.*<sup>(14)</sup> with reference to growth of Ge over Si (001). It has been shown, both by experimental observations and simulation, that some of the hut clusters continue to grow, change shape and become domes, whereas others reduce in size and disappear. Thus over a period of growth a bimodal size distribution is observed, where both hut clusters and domes can be seen, though of distinctly different sizes and shapes. Ultimately, a steady state is reached where only domes are present which attain a maximum size beyond which growth is not possible without dislocation formation. Ross, *et al.* also suggested that their model might extend to the transition of strained coherent domes to even larger dislocated islands. The transition should be similar to the hut-to-dome transition, wherein after the domes attain a maximum size some dislocate and grow in size at the cost of the others, which shrink and disappear, just like the hut clusters.

If island dimensions are smaller than the de Broglie wavelength of the charge carrier, they are called quantum dots (QDs), which are quasi-zero-dimensional systems. Due to physical confinement in three dimensions, QDs can be viewed as atom-like and are often referred to as artificial atoms. Theoretical studies of these structures are quite advanced. Indeed, in many cases the mathematical techniques needed to analyze QDs were discovered long before – in some cases many decades before – the structures were first created.

It has been suggested that QDs could solve many problems in physics and engineering, as well as provide a testbed for many scientific principals.<sup>(15)</sup> Simple problems that normally appear only in the classroom, including rectangular and parabolic quantum wells binding one or more charged particles, could be investigated using QD systems. QDs could also offer a unique opportunity to study low-dimensional paradigms, such as Landau quantization of motion of a single electron, and the radiative recombination of a few-particle system.<sup>(15)</sup>

A small number of these studies have in fact evolved into products. For instance, QDs have found application in semiconductor lasers, where they narrow spectral emission and can be tuned by an applied magnetic field. However, a much broader range of technological proposals linger, awaiting an experimental breakthrough in the control of island growth.

Island formation and growth of epitaxial SiGe/Si (001) films are governed by both thermodynamic and kinetic factors; parameters like growth rate, growth temperature, and Ge fraction play important roles. Many researchers have tried to modify the nucleation and growth of islands using surface lithography and surfactant effects.<sup>(16-23)</sup> Kammins, *et al.* and Jin, *et al.* have separately demonstrated the ability to spatially control the nucleation of Ge islands over Si mesas formed by nanoimprinting and selective epitaxy, respectively. Several surfactants like Sn, Sb, Bi and B control island formation by affecting their size and number density. Wakayama, *et al.*<sup>(24)</sup> demonstrated a multi-step procedure involving a sub monolayer C deposition step to control the structure, size and density of Ge dots on Si (001).

In this work, the goal is to guide the nucleation of islands by modification of the Si (001) surface using *ex situ* and *in situ* Ga<sup>+</sup> focused ion beams. Using the focused ion beam (FIB) we have the ability to modify the substrate in three distinct ways: morphology, surface damage and amorphization, and chemical effect. Often these three phenomena are interrelated, and separating the effects poses a challenge. Previously published work by Kammler, *et al.*<sup>(25)</sup> demonstrated the ability to control formation of Ge dots using an *in situ* FIB. However, their work relied on the use of chemical vapor deposition (CVD), which fundamentally differs from MBE-based techniques we are using. In addition the parameter space (Ga<sup>+</sup> dose and capping layer thicknesses) of the research reported here is of a greater magnitude – as will be clear during this report.

## II: INSTRUMENTATION:

A FIB column works by extracting a small amount of liquid metal through a capillary-like tube, which is then ionized and accelerated by a high voltage (10s of kV) towards the specimen. The beam of ions is then truncated and focused using mechanical apertures and E-field octupole lenses. Upon reaching the surface, the ions sputter away existing material and implant themselves. Ejected particles include secondary electrons, neutral atoms, and ions. Generally, secondary electrons are collected by a channel electron multiplier and used to produce a secondary electron image. The ion beam rasters across the surface of the sample and a secondary electron image of the surface is produced, in a manner similar to that of a scanning electron microscope (SEM). Each impinging ion knocks off a number of sample atoms, thus physically milling the sample atom-by-atom. FIB processing may alter island formation in at least four ways: the surfactant effect of Ga<sup>+</sup>, doping effects of subsurface Ga<sup>+</sup>, crystalline damage, and creation of surface morphology.

In our work, we used two separate FEI FIB columns to modify the substrate: one *in situ* FIB incorporated into the MBE system and an *ex situ* FIB. The *in situ* FIB is an FEI model that uses two octupole lenses and a fixed aperture rather than a varied physical mechanical aperture to focus the beam and truncate beam current from 1pA to ~8nA. This model has a maximum accelerating voltage of 25keV, minimum beam size in the order of 10nm, and a maximum field of view of ~1mm<sup>2</sup>. The *ex situ* FIB is an FEI 200 model, which works with an accelerating voltage of 30keV. Different beam currents can be selected by an automatic variable aperture strip (AVA) placed high in the column, with a range of 1pA to 11.5nA. The minimum beam diameter for this FIB is ~10nm using a 1pA beam current. The field of view in the FIB is divided into an array of 1024x1024 pixels, each pixel being addressable individually, thus giving precise control of the region to be fabricated.

Our laboratory is equipped with a unique and highly capable dual growth chamber MBE system (figure 1). The right chamber of this system is intended for e-gun based growth of SiGe. Wafers as large as 150mm diameter may be used. The base pressure in the chamber prior to growth was typically 2x10<sup>-10</sup>Torr. The *in situ* FIB is located in the central preparation chamber to prevent any deposition from damaging the column. The FIB and its sample stage are mounted on a bellows-isolated flange that is bolted to the lab floor, thus largely independent of the MBE system's cryopump vibrations.

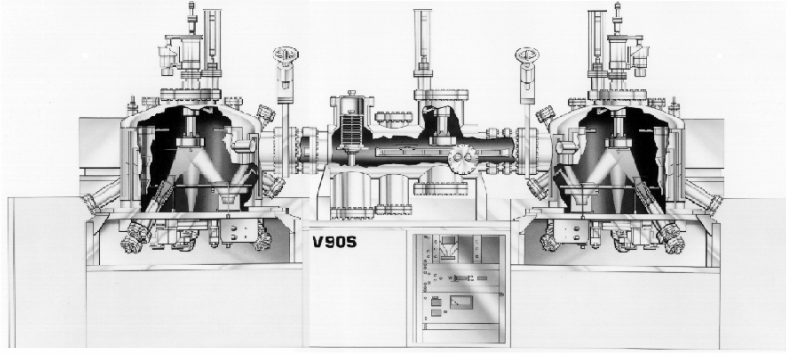


**Figure 1:** Dual VG 90s MBE system used in these experiments. The main deposition chamber on the far right and the FIB installed in the preparation chamber in the center.

### III: EXPERIMENTAL PROCESS

The purpose of this work was to investigate the effect of increasing Ga implantation and milling on the Ge islanding process. In addition we explored how burial of the milled region in a capping layer affects these results. To this end we performed experiments as follows.

For *in situ* FIB-based experiments the sample was cleaned using the Piranha clean (P-clean), which leaves an H-terminated surface. The sample was then introduced into the chamber and heated to 775°C to desorb the hydrogen. This was followed by deposition of a 100nm Si capping layer prior to milling. The sample was then moved to the preparation chamber where the FIB is installed. A matrix of nine squares with incrementally increasing doses of Ga<sup>+</sup> were implanted, each with an area 10x10μm. Doses ranging from ~10<sup>13</sup> to ~10<sup>18</sup> ions/cm<sup>2</sup> were used. In this procedure the deposition chamber has a typical base pressure of 2x10<sup>-10</sup>Torr with milling taking place at a typical base pressure of 1x10<sup>-9</sup>Torr in the prep chamber; therefore the sample never leaves UHV. After milling, 10ML of Ge were grown at 750°C and a rate of 0.4Å/sec, which leads to the formation of islands. Figure 3 (*in situ*) details this sequence: a) P-clean; b) *in situ* anneal; c) 100nm Si buffer layer deposition; d) FIB patterning; e) 10ML Ge deposition.

The *ex situ* fabrications were performed under HV conditions (10<sup>-6</sup> Torr range). The FIB was used to pattern eight separate 5x5μm areas with increasing doses of Ga<sup>+</sup> ranging from 7.5x10<sup>13</sup> to 1.05x10<sup>17</sup> ions/cm<sup>2</sup>. Figure 2 shows AFM images of the regions after FIB fabrication. We see that at the lower doses the surface swells giving a height increase of 1-2nm. This can possibly be attributed to the increased volume of the amorphized silicon, which has been previously observed.<sup>(26, 27)</sup> At increased doses, the milling effect was evident, with an observed depth of ~ 31nm for the highest dose of 1.05x10<sup>17</sup> ions/cm<sup>2</sup>.

After the FIB fabrication and AFM imaging, the sample was cleaned using a P-clean, which leaves a hydrogen-terminated surface. The sample is then introduced into the chamber and heated to 775°C to desorb the hydrogen, followed by deposition of a Si capping layer while cooling down to the growth temperature of 750°C. Then 10ML of were grown at a rate of 0.4Å/sec. Figure 3 (*ex-situ*) details this sequence: a) P-clean; d) FIB patterning; a) second P-clean; b) *in situ* anneal; c) variable thickness Si capping layer deposition; e) 10ML Ge deposition. The resultant growths from both techniques were examined using a Digital Instruments 3100 dimension AFM.

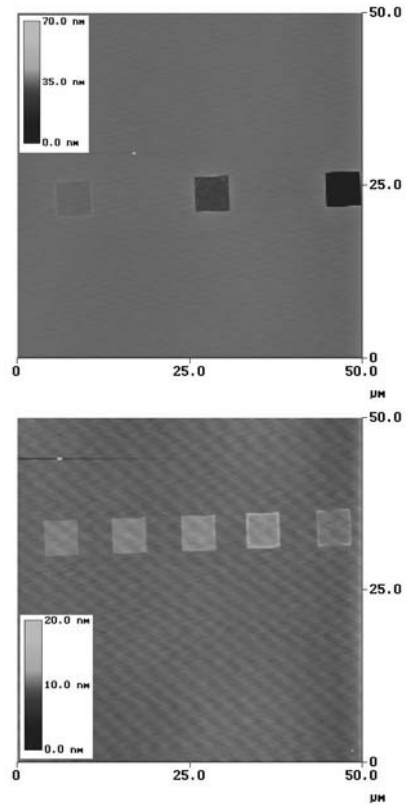


**Figure 2:** AFM images of FIB modified regions prior to MBE growth show a 1-2nm height increase in patterned regions for light doses

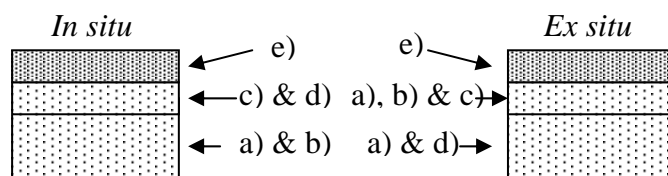


**Figure 3:** A depiction of the experimental process with order of occurrence progressing from bottom to top. a) P-Clean; b) *in situ* anneal; c) Si deposition; d) FIB patterning; e) Ge deposition.

#### IV: RESULTS:

##### IVa: *IN SITU* WITHOUT CAPPING LAYER

*In situ* studies clearly showed a  $\text{Ga}^+$  dose-dependant phenomenon. Figure 4 illustrates the drastic effect of  $\text{Ga}^+$  on island morphology at a boundary between an area that received a moderate  $\text{Ga}^+$  dosage ( $\sim 10^{15}$  ions/cm<sup>2</sup>, left) and an area that received none at all (right). This interface is characteristic for our results. We see taller islands, with a higher number density, in regions treated with  $\text{Ga}^+$ , when compared with untreated regions. Between these two regions we see a denuded zone, typically a few microns in width.

When combined into a matrix of increasing doses, Figures 5a and 5b, additional effects of  $\text{Ga}^+$  on island nucleation are observed. In the first square, which is visually missing from the pattern, the dose of  $2 \times 10^{13}$  ions/cm<sup>2</sup> did not alter the local distribution of islands. However, as the dosage increases effects begin to appear. In the second square, with a dose of  $\sim 10^{14}$  ions/cm<sup>2</sup>, a denuded zone begins to grow and island number density is increased at the interface. The middle squares, with doses of  $5 \times 10^{14}$  to  $5 \times 10^{15}$  ions/cm<sup>2</sup>, show a continued expansion of the denuded zone and increase in island density. This trend continues until significant milling begins to occur at a dose of  $\sim 10^{16}$  ions/cm<sup>2</sup>, depicted by a deepening central depression in the milled regions. As this pit continues to deepen, the denuded zone shrinks, and islanding in the milled region basically vanishes. Figure 5c zooms in on a scan where the  $\text{Ga}^+$  dose of  $5 \times 10^{13}$  ions/cm<sup>2</sup> is just beginning to create a denuded zone.

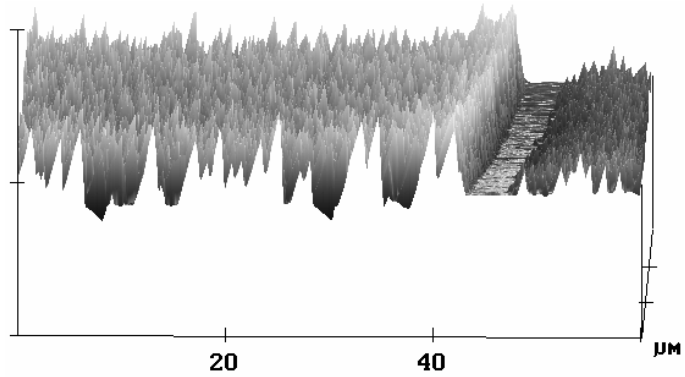


**Figure 4:** Increased island height and number density in the implanted region (left); Normal island growth separated by a few micron wide denuded zone for the untreated region (right).

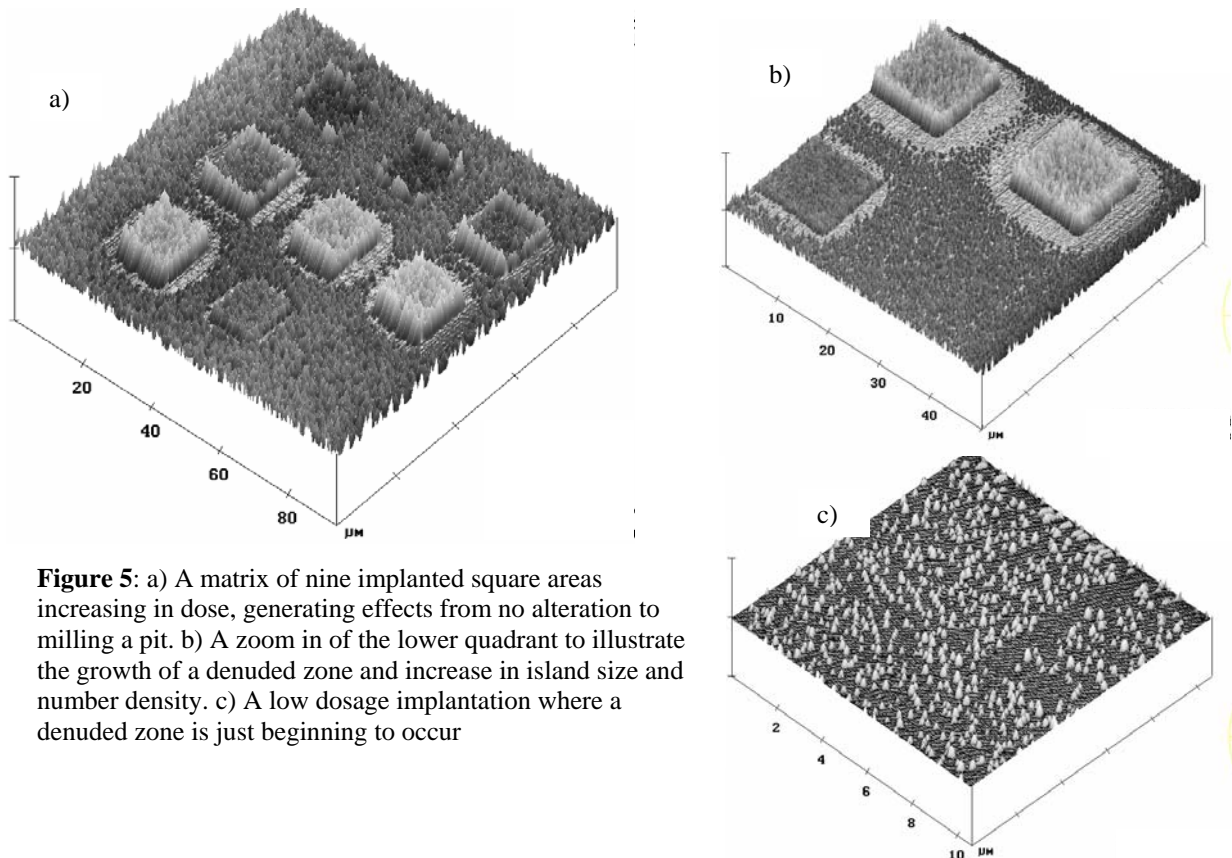


**Figure 5:** a) A matrix of nine implanted square areas increasing in dose, generating effects from no alteration to milling a pit. b) A zoom in of the lower quadrant to illustrate the growth of a denuded zone and increase in island size and number density. c) A low dosage implantation where a denuded zone is just beginning to occur

IVb: *EX SITU* WITH 10-100nm INTERMEDIATE CAPPING LAYERS

Despite thorough cleaning and an in-situ anneal, contamination may still linger on the sample surface and dominate island nucleation processes. This is evident by the fact that transmission electron microscopists are always able to image small imperfections at the boundary between substrate and epi layers (regardless of the epi growth technique). In our situation, these lingering contaminants/imperfections, could wash out the effect of the ex-situ FIB patterning (where the sample is transferred in air between buildings before insertion into the MBE apparatus). To avoid this problem, a thin Si MBE layer was first grown over the FIB patterned surface, prior to initiation of Ge growth. This layer is not present in the in-situ FIB samples above. Further, there is the possibility that the now slightly buried FIB modified layer will no longer influence Ge island nucleation. To investigate this tradeoff, we performed a series of growths using our *ex situ* conditions with varied capping layer thicknesses of 10, 30, and 100 nm.

When the capping layer thickness was 10nm results tended to mirror the findings of the *in situ* studies, as seen in figure 6. The Ga<sup>+</sup>-modified 5x5μm region can be recognized, even at the lowest Ga<sup>+</sup> dose (7.5x10<sup>13</sup>ions/cm<sup>2</sup>) for which no elevation steps were apparent. This modified region was distinguishable from the rest of the sample in two ways: 1) The affected region had a greater density of larger dots (250 to 300nm in diameter), whereas outside the region dot size tended towards 220nm; 2) The surface between the islands in the implanted regions appeared slightly rougher than the surface of non-implanted regions. At a higher dose (8.25x10<sup>14</sup>ions/cm<sup>2</sup>) we observed a row of islands bordering the implanted region. At doses 8.75x10<sup>15</sup> ions/cm<sup>2</sup> denuded zones surrounding the implanted regions formed beyond the bordering islands. These denuded zones became narrower on further increase in Ga<sup>+</sup> dosage.

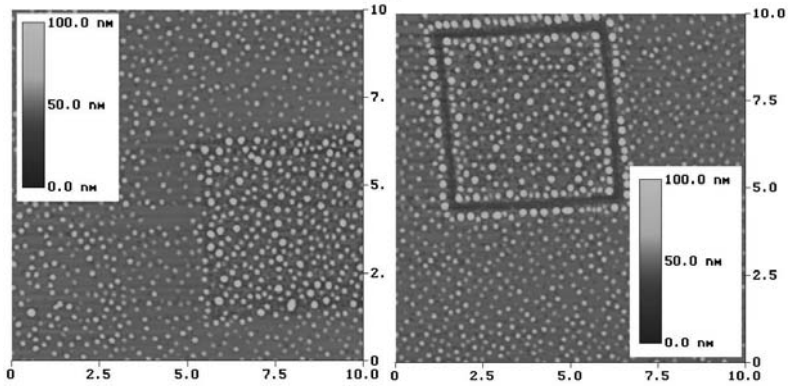


**Figure 6:** At low doses - 7.5x10<sup>13</sup>ions/cm<sup>2</sup> (L) & 8.25x10<sup>14</sup>ions/cm<sup>2</sup> (R) and low capping layer thickness (10 nm), *ex situ* experiments compare well with *in situ* growths

For samples with thicker capping layers (30nm and 100nm), growth modification could not be observed for doses below 8.25x10<sup>14</sup>ions/cm<sup>2</sup>. In contrast, figure 7 shows that FIB doses of 3.57x10<sup>15</sup> ions/cm<sup>2</sup> are sufficient to cause morphological changes for all capping layer thicknesses. FIB modified regions have larger islands for both 10nm and 30nm capping layer thicknesses. For a 100nm capping layer, large clustered islands and significant pitting mark the implanted region; this phenomenon was also seen for 10nm and 30nm capping layers at higher doses. For very high doses (1.05x10<sup>17</sup>ions/cm<sup>2</sup>) the pitting and clustering of islands was not seen; instead a low density of islands is observed in the implanted region (Figure 8).

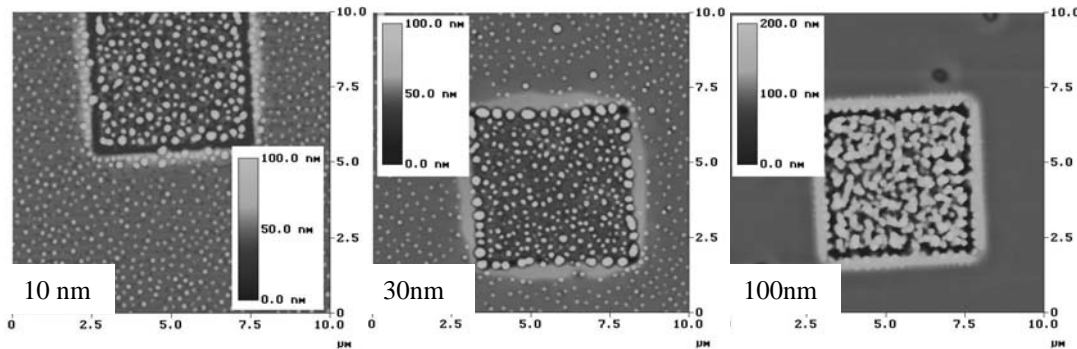


**Figure 7:** Increasing capping layer thicknesses for a mid level dose, 3.57x10<sup>15</sup>ions/cm<sup>2</sup>

Surface morphology adjacent to implanted regions was also strongly affected by FIB dose and capping layer thickness. For thicker capping layers, denuded zones seemed to appear at lower doses compared to 10nm

capping layer. Figure 7 shows a prominent denuded region for 100 nm capping layer thickness at a dose of  $3.57 \times 10^{15}$  ions/cm<sup>2</sup>. After appearance, the denuded zones seem to follow a trend similar to that for 10nm capping thickness, and decrease with increasing dose. All higher doses showed large islands bordering implanted regions.

## V: SUMMARY

We have shown that Ga<sup>+</sup> doses as low as  $5 \times 10^{13}$  ions/cm<sup>2</sup> (equivalent to 1/100<sup>th</sup> of a monolayer) affect island nucleation. Thus, large scale guided islanding can result from brief milling, making this a commercially attractive technology. For *in situ* FIB-based experiments, we observed several effects of increasing Ga<sup>+</sup> dosage: 1) within implanted regions, island height and density increased. 2) Denuded zones adjacent to implanted regions grow in size. 3) Following significant milling, the previous effects are suppressed and islanding breaks down in the implanted region. *Ex situ* experiments mirrored the above results for thin Si caps (10nm). Although the effects of low Ga<sup>+</sup> dose disappear with subsequent capping, more moderate doses of  $10^{15}$  ions/cm<sup>2</sup> and greater have effects that persist even when buried by 100nm silicon cap. This implies that guided nucleation of Ge islands on Si by Ga<sup>+</sup> focused ion beams, whether *in situ* or *ex situ*, is a versatile technique that offers great potential for realizing technological applications for quantum dots.

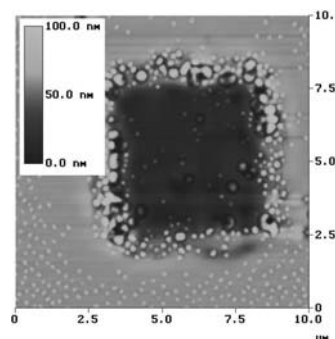


**Figure 8:** High dose,  $1.05 \times 10^{17}$  ions/cm<sup>2</sup>, with a 100nm capping layer.

## VI: ACKNOWLEDGEMENTS

This work was funded by NSF-DMR through the NSF-MRSEC at UVa, “The Center for Nanoscopic Materials Design”

## VII: References

1. W.K. Liu, and M.B. Santos, *Thin Films, Heteroepitaxial systems*, (Chapter 1.1.2)
2. W.K. Liu, and M.B. Santos, *Thin Films, Heteroepitaxial systems*, (Chapter 2)
3. J.P. Dismukes, L. Ekstrom, R. J. Paff, *J. Phys. Chem.* **68**, 3021 (1964).
4. R.Hull, J.C.Bean, *Jour. Vac. Sci. Tech. A* **7**, 2580 (1989).
5. A. Braun, K. M. Briggs and P. Böni, *Journal of Crystal Growth*, **241**, 1-2, (2002)
6. E. Kasper, *Applied Surface Science*, **102**, (1996).
7. R. People, J.C.Bean, *Applied Physics Letters* **47**, 322, (1985); **49** 229, (1986).
8. R.M. Tromp and F. Ross, *Annu. Rev. Mater. Sci.* **30**, 431 (2000).
9. R.M. Tromp, F. Ross and M.C. Reuter, *Phys. Rev. Let.* **84**, 4641 (2000).
10. Y.W. Mo, D.E. Savage, B.S. Swartzentruber and M.G. Lagally, *Phys. Rev. Let.* **65**, 1020 (1990).
11. J.A. Floro, E. Chason, *et al.*, *Physical Review B*, **59**, 1990, (1999)
12. M. Tomitori, K. Watanabe, M. Kobayashi, and O. Nishikawa, *Appl. Surf. Sci.* **76/77**, 322 (1994).
13. Gilberto Medeiros-Ribeiro, Alexander M. Bratkovski, Theodore I. Kamins, Douglas A. A. Ohlberg, and R. Stanley Williams, *Science* **279**, 353 (1998).
14. F.M. Ross, J. Tersoff and R.M. Tromp, *Phys. Rev. Let.* **80**, 984 (1998).
15. L. Jacak, P. Hawrylak, A. Wójs, *Quantum Dots*, Springer-Verlag, Berlin Heidelberg, Germany (1998).
16. T. I. Kamins, D. A. A. Ohlberg, R. Stanley Williams, *et al.*, *Applied Physics Letters*, **74**(12), 1773-1775 (1999).
17. L. Vescan, T. Stoica and B. Holländer, *Materials Science and Engineering B*, **89**, 49-53 (2002).
18. G. Jin, J.L. Liu, *et al.* *Thin Solid Films*, **369**, 49-54 (2000).
19. M. Katayama, T. Nakayama, *et al.*, *Physical Review B*, **54**(12), 8600-8604 (1996).
20. A. Portavoce, F. Volpi, *et al.*, *Thin Solid Films*, **380**, 164-168 (2000).
21. X.W.Lin *et al.*, *Physical Review B*, **52**(23), 16581-16587 (1995).
22. X. Zhou, B. Shi, *et al.*, *Thin Solid Films*, **369**, 92-95 (2000).
23. H. Takamiya, M.Miura, *et al.*, *Thin Solid Films*, **369**, 84-87 (2000)
24. Y. Wakayama, G. Gerth, *et al.*, *Journal of Crystal Growth*, **231** 474-487 (2001).
25. M. Kammler, R. Hull, M.C. Reuter, F.M.Ross, *Applied Physics Letters*, **82**(7), 1093-1095 (2003).
26. J.B. Wang, A Datta, Y.L. Wang, *Applied Surface Science*, **135** 129-136 (1998).
27. C. Lehrer, L. Frey, *et al.*, *J. Vac. Sci. Technol. B*, **19**(6), 2533-2537 (2001).